日本創外固定・骨延長学会雑誌18：127　2007

超音波エコートラッキング法を用いた骨癒合判定法

東京大学医学部整形外科
松山順太郎・大西五三男・別所 雅彦・大橋 暁・松本 卓也・中村 耕三
アロカ株式会社
酒井 亮一・鈴木 浩之・大塚 利樹・宮坂 好一・原田 烈光

A new method for evaluation of fracture healing by echo tracking

骨癒合判定は今なおX線写真による定性的な方法に依存しているが，最も重要な要件は力学強度の回復を検出することである。本研究の目的は，骨癒合を非侵襲に精確且つ定量的に判定し，創外固定器の抜去時期の決定を可能とする方法を確立することである。骨の荷重に対する変形を定量的に検出し，骨の力学特性を評価することにより骨癒合を評価することが可能である。骨の微小変形の検出を達成するために超音波のエコー信号の位相変化を測定するエコートラッキング（ET）法を用い，2.6μmの測定精度で計測可能な診断装置を開発した。本装置を用い，単支柱式創外固定器による下腿延長術を行った患者に対し骨癒合の判定を行った。座位の状態にて，膝上から徒手的に100Nの縦圧縮荷重を加え，延長仮骨部の変形量を測定した。超音波プローブを創外固定器の支柱に固着し，プローブ長軸上の直線4cmの間隔に5点のトラッキングポイントを設け同時計測し，各点の変位測定から変形量（ETS）を抽出し定量評価した。対象は軟骨無形成症・軟骨低形成症の4名6肢で平均年齢は16歳であった。骨硬化期間初期より創外固定器抜去まで，2～6週間隔で測定を実施した。測定期間は平均21.2週で測定回数は平均6.1回であった。いずれの症例においてもET測定による変形量（ETS）は経時的に指数関数的減少を示し，仮骨部の剛性変化を定量検出可能であった。また，創外固定器抜去前の最終測定時には，いずれの症例も500 ETS以下であった。荷重と抜重における荷重・変形量のグラフでは，粘性を示すヒステリシスループが描出され，経時的な粘性の減少が検出可能であった。ET計測により非侵襲に仮骨部の剛性・粘性が検出可能であり骨癒合の進行が定量評価可能であった。今後，創外固定器症例の許容荷重量の決定・抜去時期を判断する診断法として応用可能であると考える。

43

CT・CAD/有限要素法解析を用いた創外固定ピン応力の検討
ー非対称ピンプロファイルはピンと骨の界面における応力集中を軽減するー

Stress analysis of the external fixator pin cluster using a patient specific CT-CAD/FEM
-Asymmetrical pin thread profile can reduce pin-bone interface stress concentration-

東京大学医学部整形外科

○ 大腿 暁、大西 五三男、別所 雅彦、松本 卓也、松山 順太郎、中村 耕三

創外固定においてピン刺入部の応力を検討するために、患者CTデータを基に有限要素法解析を行った。大腿骨骨折患者に対し非骨折側大腿骨のCT撮影を行い、骨幹部中央を骨折部として大腿骨骨折有限要素モデルを作成した。骨は不均質材料とし材料特性は各要素の位置に対応するCT値から個々に算出した。固定ピン4本を大腿骨に刺入し支柱により架橋する構造をCAD dataを基に創外固定モデルとして作成した。大腿骨頭より機能軸方向へ荷重を加え大腿骨遠位端を完全拘束し弾性解析を行った。最近位および最遠位のピン(アウターピン)には引張優位な応力が、骨折部に近接するピン(インナーピン)には圧縮優位な応力がピン刺入部に存在した。全てのピンにスレッド形状が対称のピン($\beta=\gamma=22.5°$)を用いたモデル(対称ピンモデル)とアウターピンにtype Aピン($\beta=40°$, $\gamma=5°$)、インナーピンにtype B($\beta=5°$, $\gamma=40°$)の非対称ピンをそれぞれ用いたモデル(非対称ピンモデル)について弾性解析を行った。ピン刺入部の最大相当応力が対称ピンモデルよりも非対称ピンモデルの方が低下していた。非対称ピンを最適位置に刺入することで個々のピンおよび創外固定全体の骨折固定力が向上すると考えられる。

23 CT/有限要素法による脊椎椎体の強度解析 —日常生活における骨強度評価への応用—

東京大学医学部整形外科
○松本　卓也、大西　五三男、別所　雅彦、大橋　暁、飛田　健治、中村　耕三

【目的】骨粗鬆症の評価は主にDXA法が用いられるが、骨強度が定量測定できないという限界がある。第6回本学会において今井らによりCT/有限要素法により椎体の単軸圧縮強度が精確に評価できると報告した。これをふまえ、同方法を応用し日常生活動作における骨強度、すなわち日常生活動作における荷重条件での骨強度評価を行うことを目的とした。【対象と方法】対象は未治療の原発性骨粗鬆症女性患者7名、平均年齢60歳。倫理委員会の承認のもと、患者の同意を得て、第2腰椎の定量的CT撮影を行い、CTデータより有限要素法による強度解析を行った。CT/有限要素法による強度解析は定量的CTのDICOMデータから、3次元骨強度解析モデルを作成した。荷重条件・拘束条件は、椎体上面を垂直圧縮し、椎体下面を完全拘束した単軸圧縮モデル（Imai, 2006）、立位・前屈位における椎体への過重負荷分布（Pollintine, 2004）を応用した。すなわち立位時には椎体の前方1/3：中央1/3：後方1/3を19：31：41に、前屈時には59：48：38に分配した荷重を椎体上面に、椎体下面を完全拘束した立位荷重、前屈位荷重モデルについて解析を行い、骨強度予測を行った。【結果】予測骨折荷重は単軸圧縮と立位荷重の条件では相関係数0.913、回帰直線の傾き0.924、単軸圧縮と前屈位荷重の条件では相関係数0.863、回帰直線の傾き1.360であった。前屈荷重の予測強度は7例中4例で単軸圧縮予測強度より低く、前屈位での予測骨折荷重が低い症例では、立位／前屈位の予測骨折荷重比が変わらない症例に比べ、前方の皮質骨シェルおよび皮質骨シェル近傍の海綿骨の骨密度が低い傾向にあった。骨折荷重時の最小主ひずみ分布は単軸圧縮に比べ立位荷重では後方に、前屈位荷重では前方に圧縮ひずみ分布が広くなる傾向があった。【考察】単軸圧縮における予測強度は立位荷重における予測強度とほぼ同等と考えられた。前屈荷重の予測強度が低い事は、骨粗鬆症における椎体の骨折リスクの評価において、骨密度分布や骨形態などの骨強度だけでなく、椎体に加わる荷重の方向にも依存する事を示しており、骨折が起こりやすい荷重方向を見極め、骨折リスクを考慮した生活指導が出来れば高齢者の骨折予防への一助となりうる。【結論】CT/有限要素法による強度解析を日常生活動作における骨強度評価に応用した。今後は後方要素の考慮など解析モデルの完成度を高め、症例を増やし本法の有用性を検討したい。

24 CT画像を用いた有限要素法非線形解析による大腿骨近位部の骨強度評価—荷重・拘束条件の相違による予測骨強度の相違について—

東京大学医学部整形外科
○別所　雅彦、大西　五三男、松本　卓也、大橋　暁、飛田　健治、松山　順太郎、中村　耕三

【目的】高齢者の大腿骨近位部骨折の危険予測は画像診断や骨密度測定にて行われるが、これは骨粗鬆の程度は評価するが、構造的強度を評価できない。大腿骨近位部骨折患者に対し、非骨折側の大腿骨の3次元CT有限要素解析を行い、荷重方向の相違による骨折荷重を検討した。本法が大腿骨近位部骨折の有用な危険予測法となり得るか検討した。【方法】対象は、80歳代の女性の大腿骨近位部骨折患者23名（平均85.2歳）。受傷後1週間以内に定量的CTを撮像し、非骨折側の3次元解析モデルを作成した。各要素の材料特性は各要素位置に対応するCT値から骨密度を個々に算出し、骨密度に対応する材料特性を割り当てた。荷重拘束条件は、立位を模擬した条件と側方転倒・後側方転倒を模擬した条件を設定した。Newton-Raphson法を用いた荷重増分法による非線形解析を行い、予測骨折荷重を解析した。各荷重拘束条件の相違による強度の相違を比較した。統計処理は、Pearson's test、ANOVA法、Post hoc testにFisher's PLSD法を用いた。有意水準を0.05以下とした。【結果】予測骨折荷重は、立位条件3080N（標準偏差(SD)550N）、側方転倒条件1040N（SD236N）、後側方転倒条件700N（SD167N）であった。立位条件の予測骨折荷重は、側方・後側方転倒条件よりも有意に大きかった($p<0.001$)。側方転倒条件での予測骨折荷重は、後側方転倒条件よりも有意に大きかった($p<0.001$)。立位条件と側方転倒条件での予測骨折荷重の相関性は、$r=0.52$（$p=0.01$）、立位条件と後側方転倒条件では、$r=0.55$（$p=0.006$）、側方転倒条件と後側方転倒条件では、$r=0.67$（$p<0.001$）であった。【考察、結論】立位条件よりも側方転倒条件、側方転倒条件よりも後側方転倒条件が骨折危険度を高めた。また、各荷重・拘束条件間の予測骨折荷重の相関は有意であるが、相関性は低かった。大腿骨近位部の骨強度評価は、複数の荷重拘束条件から評価する必要性があると示唆された。

07(IX)-39

新鮮死体大腿骨標本の CT/有限要素法による予測骨折荷重の正確性の検証

○ 別所 雅彦[a]、大西 五三男[a]、松本 卓也[a]、大橋 暁[a]
飛田 健治[a]、中村 耕三[a]
[a]東京大学整形外科

Prediction of the strength of the proximal femur by a CT based finite element method

M. Bessho[a], I. Ohnishi[a], T. Matsumoto[a], S. Ohashi[a], K. Tobita[a], K. Nakamura[a]
[a] *The Department of Orthopaedic Surgery, The University of Tokyo, Tokyo, Japan*

Abstract: Hip fractures are the most serious complication of osteoporosis and have been recognized as a major public health problem. In elderly persons, hip fractures occur as a result of increased fragility of the proximal femur due to osteoporosis. It is essential to precisely quantify the strength of the proximal femur in order to estimate the fracture risk and plan preventive interventions. CT based finite element analysis could possibly achieve precise assessment of the strength of the proximal femur. The purpose of this study was to create a simulation model that could accurately predict the strength of the proximal femur using a CT based finite element method and to verify the accuracy of our model by load testing using fresh frozen cadaver specimens. Eleven right femora were collected. The axial CT scans of the proximal femora were obtained with a calibration phantom, from which the 3D finite element models were constructed. Non-linear finite element analyses were performed. A quasi-static compression test of each femur was conducted. Fracture loads of the prediction significantly correlated with those measured (r = 0.97).
Key words: Finite element method, Bone strength, Osteoporosis, Fracture load, Femur

1. 目的

骨粗鬆症が原因である大腿骨近位部骨折の患者は、近年、発生件数が年間約 12 万人となり、1987 年から比較すると、1992 年で 1.7 倍、2002 年で 2.2 倍となっており、年々確実に増えている[1]。現在の骨強度評価は、主に X 線写真および DXA(dual energy X-ray absorptiometry)による骨密度で評価されている。DXA 法による骨密度測定は、骨の立体的構造強度を定量評価できないという限界がある。こうした背景から、CT/有限要素法を用いて、骨強度を定量的に評価できる解析モデルの開発を行った。解析モデルの精確性の評価を行うために、新鮮凍結死体標本の圧縮試験を行った。前回[2]、主ひずみの実験と解析の結果の相関が、r = 0.963 と高く、主ひずみを正確に評価できることを報告した。今回は、骨折荷重値の実験値と解析値の比較検討を行った。

2. 対象と方法

男性 5 人(30～90 歳 平均 56.8 歳)、女性 6 人(72～85 歳 平均 72.8 歳)から摘出した右大腿骨 11 本を使用した。倫理審査委員会の承認をへて遺族への説明同意を得た後に、死後 12 時間以内に採取し、実験まで凍結保存した。ＣＴ画像、軟Ｘ線にて摘出大腿骨に骨折、ガン転移などの骨病変がないことを確認した。大腿骨は、小転子中央から遠位に 14ｃｍの部分で骨幹部を切断した。レジストレーション用にエポキシ樹脂マーカーを計 11 個、貼り付けた。ＣＴ (Aquilion Super 4、東芝メディカルシステムズ)を用いて、骨量ファントム (B-MAS200, 京都科学) とともに、検体を 3mm スライスで撮影を行った。圧縮試験は、大腿骨骨軸 20 度傾けて骨頭に対して準静的に圧縮を行った(Fig. 1)。一方、定量的 CT から、海綿骨に 3mm の 4 節点ソリッド要素と、皮質骨外層に 0.4 mm の 3 節点シェル要素を使用し、3 次元骨強度解析モデルを作成した(Fig. 2)。骨は不均質材料とし、重量密度は各要素に対して骨量ファントムの CT 値から換算式により計算した。材料特性は各要素の位置に対応する重量密度から個々に算出し、これに対応する要素の材料特性に割り当てた。ヤング率は Keyak [3]ら、および Keller [4]らの方法により設定した。ポアソン比は、0.4 とした。荷重条件および拘束条件は、骨軸から 20 度内側に傾けた方向で骨

頭を圧縮し、骨幹部遠位端を拘束した条件とした。

Newton-Raphson 法を用いた荷重増分法による非線形解析を行い、1 つのシェル要素の最大主応力がその要素の臨界応力を超える場合（クラック）、または、1 つのシェル要素の Drucker-Prager 相当応力が要素の降伏応力を超え、かつ最小主歪みが-10000 micro strain 以下の場合(圧潰)をそれぞれ骨折と定義した。1 要素以上の破壊を骨折と定義し、予測骨折荷重を解析した。

骨折荷重値の実験値と解析値を比較対照した。統計学的評価は、Pearson の相関係数検定、直線回帰を行い、有意水準を $p<0.05$ とした。

Fig. 1: Uniaxial compressive loading testing

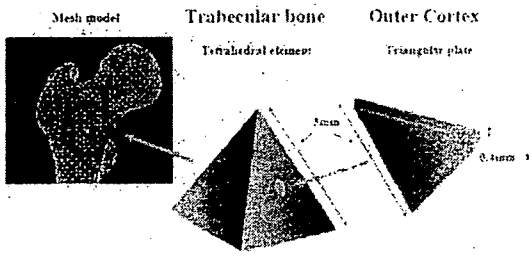

Fig. 2: Used elements

3. 結果

x 軸を解析での予測骨折荷重、y 軸を実験での骨折荷重とした回帰直線は、$y = 642 + 0.936x$、$r = 0.979$、95 %上方信頼限界は 0.920、下方信頼限界は 0.995、$P<0.0001$、SEE = 228 N であった(Fig. 23)。回帰直線傾きは明らかに 1 と差がなく($p = 0.75$)、回帰直線の切片も明らかに0と差がなかった($p = 0.08$)

4. 考察

Keyak ら[5]の非線形解析の研究では、骨折荷重の実験値と解析値の回帰直線（x 軸を解析での予測骨折荷重、y 軸を実験での骨折荷重）の傾きは 0.77、切片は 1150 N、相関係数は $r = 0.962$、95 %信頼区間は 0.899～0.986 と報告していた。また、Cody ら[6]の線形解析の研究では、相関係数は $r = 0.915$ と報告していた。95 %信頼区間は報告されていなかったが、検体数が26検体であるため0.817～0.961であった。本研究における実験の骨折荷重と予測骨折荷重の相関性は、過去の報告と比べ統計学的に非劣性であると判断できた。しかし、Keyak ら[14]の報告では、回帰直線の傾きは明らかに 1 と差があった（$p<0.001$）が、我々の解析モデルでは、傾きは明らかに 1 と差がなく回帰直線の傾きは優れていると考えられた

文献

1) Yoshimura, N., Suzuki, T., Hosoi, T. and Orimo, H., Epidemiology of hip fracture in Japan: incidence and risk factors. Journal of Bone and Mineral Metabolism 2005;23 Suppl:78-80.
2) 新鮮死体大腿骨標本のCT/有限要素法による骨ひずみ予測の正確性の検証，別所雅彦，大西五三男ら、日本コンピュータ外科学会誌 2006、8 巻 3 号 Page256-257
3) Keyak, J. H., Lee, I. Y. and Skinner, H. B., Correlations between orthogonal mechanical properties and density of trabecular bone: use of different densitometric measures. J Biomed Mater Res 1994;28:1329-36.
4) Keller, T. S., Predicting the compressive mechanical behavior of bone. J Biomech 1994;27:1159-68.
5) Keyak, J. H., 2001. Improved prediction of proximal femoral fracture load using nonlinear finite element models. Med Eng Phys 23, 165-173.
6) Cody, D. D., Gross, G. J., Hou, F. J., Spencer, H. J., Goldstein, S. A. and Fyhrie, D. P., 1999. Femoral strength is better predicted by finite element models than QCT and DXA. J Biomech 32, 1013-1020.

07(X)-43

CT/有限要素法による骨強度評価の臨床応用
－大腿骨変形治癒例に対する歩行荷重管理－

○松本卓也　大西五三男　別所雅彦　大橋暁　飛田健治　中村耕三
東京大学　整形外科

Clinical Application of a CT Based Nonlinear Finite Element Method
－Weight Bearing Control of Patients with Mal-united Fracture of the Femur－

Takuya Matsumoto, Isao Ohnishi, Masahiko Bessho, Satoru Ohashi, Kenji Tobita, Kozo Nakamura
Department of Orthopaedic Surgery, University of Tokyo, Tokyo.

Abstract: Estimation of bone strength still depends on X-ray findings. Thus, it is quite difficult to predict bone strength in patients with large defect or deformity. Bessho et al. made the precise quantitative evaluation of bone strength of cadavere femora using a CT based nonlinear finite element method. We applied this method clinically and assessed strength of mal-united femora in 2 patients, thereby controlling the magnitude of weight bearing. Post operative management in these patients was successful without any ocurrence of re-fracture in the the follow up period.

Key words: Finite element method, Bone strength, Fracture, weight bearing

背景

骨折後、変形治癒や骨欠損を伴った場合、過度な荷重歩行は再骨折につながるが、不十分な荷重歩行は骨形成に悪影響を及ぼすだけでなく骨萎縮をきたす可能性もあり、ジレンマの中で後療法での荷重決定を迫られる。骨強度の評価は今なおX線写真による定性的評価に依存し、重度外傷後の骨欠損・変形治癒例では荷重量決定に難渋する場合が多く、精度と再現性をもつ定量的な骨強度予測評価法の開発が必要である。

目的

X線による骨強度予測が困難であった大腿骨骨折後の高度変形治癒例に対し、新鮮死体標本を用いた大腿骨近位部の圧縮強度がCT/有限要素法解析で精度高く評価できた別所ら[1]の報告を元に有限要素法解析による強度予測を応用、後療法における荷重量の管理を行った。治療経過中、再骨折することなく骨強度が増加し、本法が有用であったので報告する。

対象と方法

症例は大腿骨開放骨折を含む多発外傷後、変形治癒となった2症例。

症例1　42歳　男性　現病歴交通事故による多発外傷後感染を起こし変形治癒となった。受傷後8ヶ月目、両松葉杖 touch gait で初診（Fig1 初診時レントゲン）。当科にて保存加療を行い、受傷後1年目と2年目でCT/有限要素法解析を行った。

Fig1 初診時レントゲン

CT有限要素法の解析は大腿骨全長を2ミリ厚で定量的CTデータを取得し、患側大腿骨を3次元構築、患者固有の解析モデルを作成した。立位荷重を模擬した荷重・拘束条件で有限要素法よる非線形解析で骨折荷重・部位および、歪みの予測を行った。

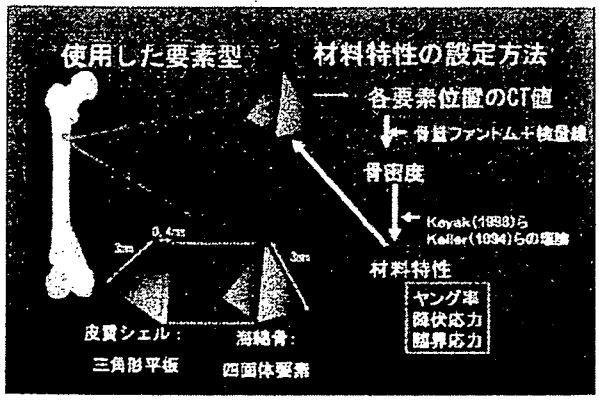

Fig2　要素型・材料特性

モデルは海綿骨が3ミリの正四面体要素、皮質骨外層が3ミリの正三角形のシェル要素で構成、材料特性は要素位置に対応するCT値から骨密度を算出しKeyak[3]、Keller[2]らの理論に基づき材料特性に変換した(Fig2)。

荷重・拘束条件は、骨頭を荷重部とし、機能軸を荷重方向として遠位端を完全拘束した片脚起立を模擬した。非線形解析を行い、予測骨折荷重を算出し、結果をもとに後療法における荷重負荷量を決定した。

経時的評価項目は評価時期を：受傷後　2年目と4年目の2回とし骨折荷重・部位、骨密度、最大・最小主歪み分布を評価、Mechanical Usage Windowを荷重指標にした。

結果

骨折荷重は初回80kgf、2回目は310kgfであった

骨折部近傍の骨密度は皮質骨周囲の骨密度が増加し、最大主ひずみが高い領域が減少、最小主が低いが低い領域も減少し、ひずみの絶対値が小さくなった。

症例2

交通事故による大腿骨遠位の粉砕開放骨折であった。創外固定器をもちいて固定したが不安定性が残りギプス固定となった。9cmの短縮、40度後方凸の角状変形が残存し、当科初診した。

受傷後3年目と4年目でCT/ 有限要素法解析を行った。

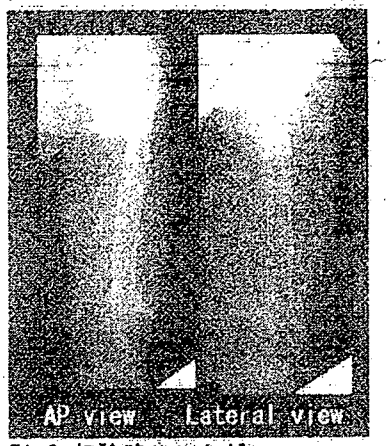

Fig3 初診時レントゲン

結果

骨折荷重は初回100kgf、2回目は250kgfであった

考察

フロスト[4]は1000-3000μstrainの歪が負荷すると、骨のmodelingにより骨量が増加すると報告した。2症例の50kgf荷重時の予測最大・最小主ひずみはTable1のようになっており、経時変化に伴い、骨のmodelingが進み歪のレベルはmild overload windowからadaptive windowに移行した。

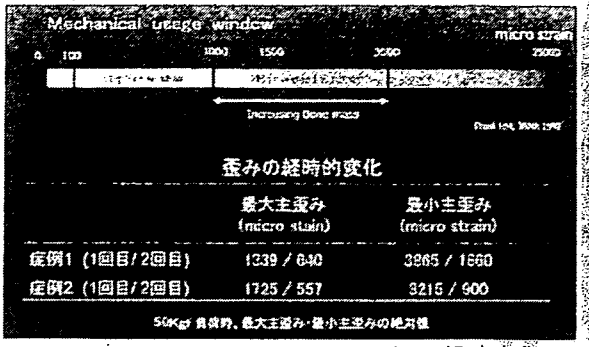

Table1 Mechanical usage window 歪み経時変化

症例1では1回目の解析後に1/3荷重としから2年後にT字杖へ　症例2では　1/4荷重から1年後に片ロフストランド杖へと荷重量を増加できた。

2症例ともに治療経過で再骨折はなかった。

結語

CT/有限要素法による骨強度予測を行ない、後療法における荷重量決定に有用であった。

文献

1.Bessho M.　*J Biomech* 2007;40:1745-53.
2.Keller TS. *J Biomech* 1994;27:1159-68.
3.Keyak JH. *J Biomed Mater Res* 1994;28:1329-36.
4.Frost HM. *J Bone Miner Res* 1997;12:1539-46

SPINE Volume 33, Number 1, pp 27–32

In Vivo Assessment of Lumbar Vertebral Strength in Elderly Women Using Computed Tomography-Based Nonlinear Finite Element Model

Kazuhiro Imai, MD, PhD,*† Isao Ohnishi, MD, PhD,* Seizo Yamamoto, MD, PhD,† and Kozo Nakamura, MD, PhD*

Study Design. *In vivo* study of a computed tomography (CT)-based nonlinear finite element model (FEM).

Objective. To establish an FEM with the optimum element size to assess the vertebral strength by comparing analyzed data with those obtained from mechanical testing *in vitro*, and then to assess the second lumbar (L2) vertebral strength *in vivo*.

Summary of Background Data. FEM has been reported to predict vertebral strength *in vitro*, but has not been used clinically.

Methods. Comparison among the 3 models with a different element size of 1 mm, 2 mm, and 3 mm was performed to determine which model achieved the most accurate prediction. Vertebral strength was assessed in 78 elderly Japanese women using an FEM with the optimum element size.

Results. The optimum element size was 2 mm. The L2 vertebral strength obtained with the FEM was 2154 ± 685 N, and the model could detect preexisting vertebral fracture better than measurement of bone mineral density.

Conclusion. The FEM could assess vertebral strength *in vivo*.

Key words: vertebral strength, osteoporosis, finite element model, elderly women, *in vivo* assessment. **Spine 2008;33:27–32**

Osteoporotic vertebral fractures have become a major social problem because the elderly population continues to increase. Vertebral fractures affect approximately 25% of postmenopausal women.[1] Measurement of the bone mineral density (BMD) by quantitative computed tomography (QCT) and dual energy radiograph absorptiometry (DXA) have been used to predict the risk of vertebral fracture. However, the correlation between vertebral bone strength and BMD measured by QCT is reported to be only 0.37 to 0.74,[2–7] while the correlation achieved with DXA is reported to be 0.51 to 0.80.[5–9] Therefore, such methods only explain 37% to 80% of vertebral strength. Bone strength primarily reflects the bone density and bone quality, which are influenced by bone architecture, turnover, accumulation of damage, and mineralization.[10]

It has been reported that a CT-based nonlinear finite element model (FEM) could predict vertebral strength and fracture sites accurately *in vitro*.[11] To predict quantitative strength and fracture sites is essential for the clinical application of an FEM because both parameters are important indicators of vertebral fracture risk. Prediction by an FEM with a smaller element size using the data from computed tomography (CT) scans with a thinner slice thickness and a smaller pixel size is thought to be more accurate. On the other hand, thinner CT slices lead to more radiation exposure in the clinical situation. To decrease radiation exposure as much as possible during CT scanning, optimization of the element size of the FEM was performed by assessing the accuracy of the FEM simulation.

The purposes of this study were to establish a CT-based nonlinear FEM with the optimum element size to predict the vertebral fracture load by evaluating the accuracy of our model from a comparison between predictions and data obtained by mechanical testing of human cadaver specimens *in vitro*, and then to assess lumbar vertebral strength in elderly women using the optimized CT-based nonlinear FEM.

■ Materials and Methods

Optimization of the Element Size of the FEM. This study used CT data and mechanical testing data obtained previously.[11] Twelve thoracolumbar vertebrae (T11, T12, and L1) with no skeletal pathology were collected within 24 hours of death from 4 men (31, 55, 67, and 83 years old). The vertebrae were disarticulated, and the discs were excised. Then the posterior element of each vertebra was removed by cutting through the pedicles. The vertebrae were immersed in water and axial CT scans with a slice thickness of 1 mm and a pixel width of 0.351 mm were obtained using a Lemage SX/E (GE Yokokawa Medical System, Tokyo, Japan) with a calibration phantom containing hydroxyapatite rods.

The 3-dimensional FEM was constructed from CT data using Mechanical Finder software (Mitsubishi Space Software Co., Tokyo, Japan). Three models with a different element size were created for each vertebra using 1 mm, 2 mm, or 3 mm tetrahedral elements. To the outer surface of the tetrahedral elements, triangular plates were attached as to form a cortical

From the *Department of Orthopaedic Surgery, School of Medicine, Tokyo University, Bunkyo-ku, Tokyo, Japan; and †Department of Orthopaedic Surgery, Tokyo Metropolitan Geriatric Medical Center, Itabashi-ku, Tokyo, Japan.

This work has been supported by the grant in aid for Scientific Research received from Japan Society for the Promotion of Science.

Acknowledgment date: March 27, 2007. Revision date: June 8, 2007. Acceptance date: July 2, 2007.

The manuscript submitted does not contain information about medical device(s)/drug(s).

No funds were received in support of this work. No benefits in any form have been or will be received from a commercial party related directly or indirectly to the subject of this manuscript.

Address correspondence and reprint requests to Isao Ohnishi, MD, PhD, Department of Orthopaedic Surgery, School of Medicine, Tokyo University, 7-3-1 Hongo, Bunkyo-ku, Tokyo 113-0033, Japan; E-mail: ohnishi-i@umin.ac.jp

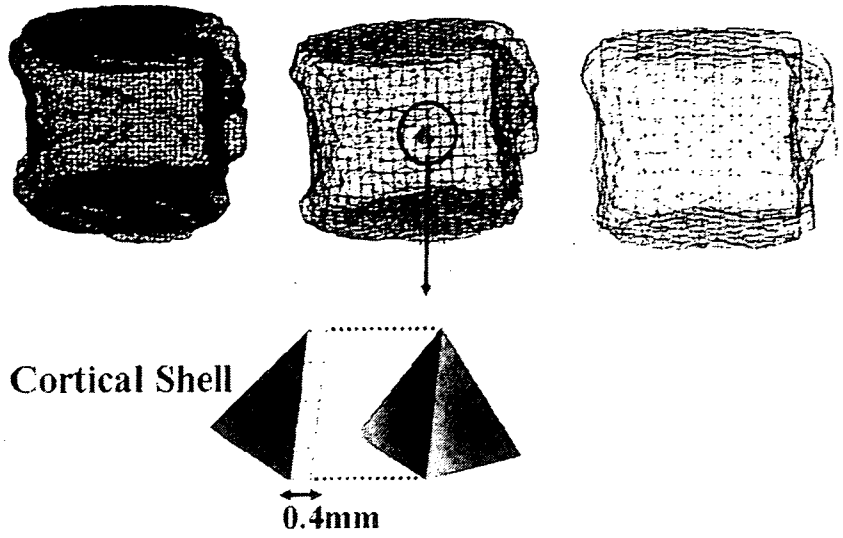

Figure 1. Finite element models of a whole vertebral body constructed with 1 mm, 2 mm, or 3 mm tetrahedral elements. The cortical shell was modeled by using triangular plates with a thickness of 0.4 mm. The model on the left consists of 104,205 nodes with 585,784 tetrahedral elements and 15,800 triangular plates constructed using 1-mm size elements. The middle model consists of 12,938 nodes with 70,022 tetrahedral elements and 3586 triangular plates constructed using 2-mm elements. The model on the right consists of 3476 nodes with 18,103 tetrahedral elements and 1330 triangular plates constructed using 3-mm size elements.

shell (Figure 1). The thickness of this shell was set as 0.4 mm based on the previous papers.[12–14]

To allow for bone heterogeneity, the mechanical properties of each element were computed from the Hounsfield unit value. Ash density of each voxel was determined from the linear regression equation created by these values of the calibration phantom. Ash density of each element was set as the average ash density of the voxels contained in one element. Young's modulus and the yield stress of each tetrahedral element were calculated from the equations proposed by Keyak *et al.*[15] Young's modulus of each triangular plate was set as 10 GPa and Poisson's ratio of each element was set as 0.4.

A uniaxial compressive load with a uniform distribution was applied on the upper surface of the vertebra and all the elements and all the nodes of the lower surface were completely restrained. Each model was analyzed using Mechanical Finder software as reported previously.[11]

A nonlinear FEM by Newton-Raphson method was used. To allow for the nonlinear phase, mechanical properties of the elements were assumed to be bilinear elastoplastic, and the isotropic hardening modulus was set as 0.05. Each element was assumed to yield when its Drucker-Prager equivalent stress reached the element yield stress. In the postyield phase, failure was defined as occurring when the minimum principal strain of an element was less than −10,000 microstrain.

The predicted fracture load was defined as the load that caused at least one element failure, while the measured fracture load was defined as the ultimate load that was achieved by mechanical testing. Pearson's correlation analysis was used to evaluate correlations between the fracture load predicted by FEM simulation and the measured fracture load. To optimize the element size of the FEM, the accuracy of prediction of the fracture load was compared among the 3 models with different element sizes. To assess the relationship between the models with a different element size, linear regression analyses were performed.

In addition, we also created models using 1.4 mm and 4.5 mm elements as well as 1 mm, 2 mm, and 3 mm elements to investigate the model convergence. For each of the models, total strain energy was calculated at a load of 1000 N, under which all specimens were in the elastic phase. Data on the total strain energy were compared among the 1 mm (average 403,033 tetrahedral elements), 1.4 mm (average 143,367 tetrahedral elements), 2 mm (average 47,687 tetrahedral elements), 3 mm (average 11,903 tetrahedral elements), and 4.5 mm (average 2719 tetrahedral elements) models.

***In Vivo* Assessment of Lumbar Vertebral Strength.** The subjects were ambulatory postmenopausal Japanese women aged 60 to 85 years. Excluded from participation were women with disorders of bone and mineral metabolism other than postmenopausal osteoporosis, those who had any recent or current treatment with the potential to alter bone turnover or bone metabolism, and those with a history of second lumbar vertebral (L2) fracture. The study protocol was approved by our ethics committee and each participant provided written informed consent. A total of 78 eligible participants were enrolled in this study.

In all the participants, the BMD (g/cm^2) of the lumbar spine (L2–L4) was measured by DXA (DPX; Lunar, Madison, WI) in the supine position and axial CT scans of L2 were obtained with a slice thickness of 2 mm and pixel width of 0.35 mm using Light Speed QX/i (GE Yokokawa Medical System, Tokyo, Japan) with a calibration phantom containing hydroxyapatite rods. The 3-dimensional FEM was constructed from the CT data using Mechanical Finder with 2 mm tetrahedral elements and 2 mm triangular plates, and the fracture load was analyzed using this software as described above.

Results are expressed as the mean ± standard deviation (SD). Statistical analysis was performed with the Mann-Whitney *U* test and the Kruskal-Wallis test. Differences were considered significant at $P < 0.05$.

■ Results

Optimization of the FEM Element Size

There was a strong linear correlation between the fracture load predicted by the FEM with 1 mm tetrahedral elements and the measured loads ($r = 0.938$, $P < 0.0001$), and the slope of the regression line was 0.934 (Figure 2A). With 2 mm elements, the correlation was even stronger ($r = 0.978$, $P < 0.0001$), and the slope of the regression line was 0.881 (Figure 2B). With 3 mm elements, the correlation was slightly weaker ($r = 0.866$, $P < 0.0001$), and the slope of the regression line was

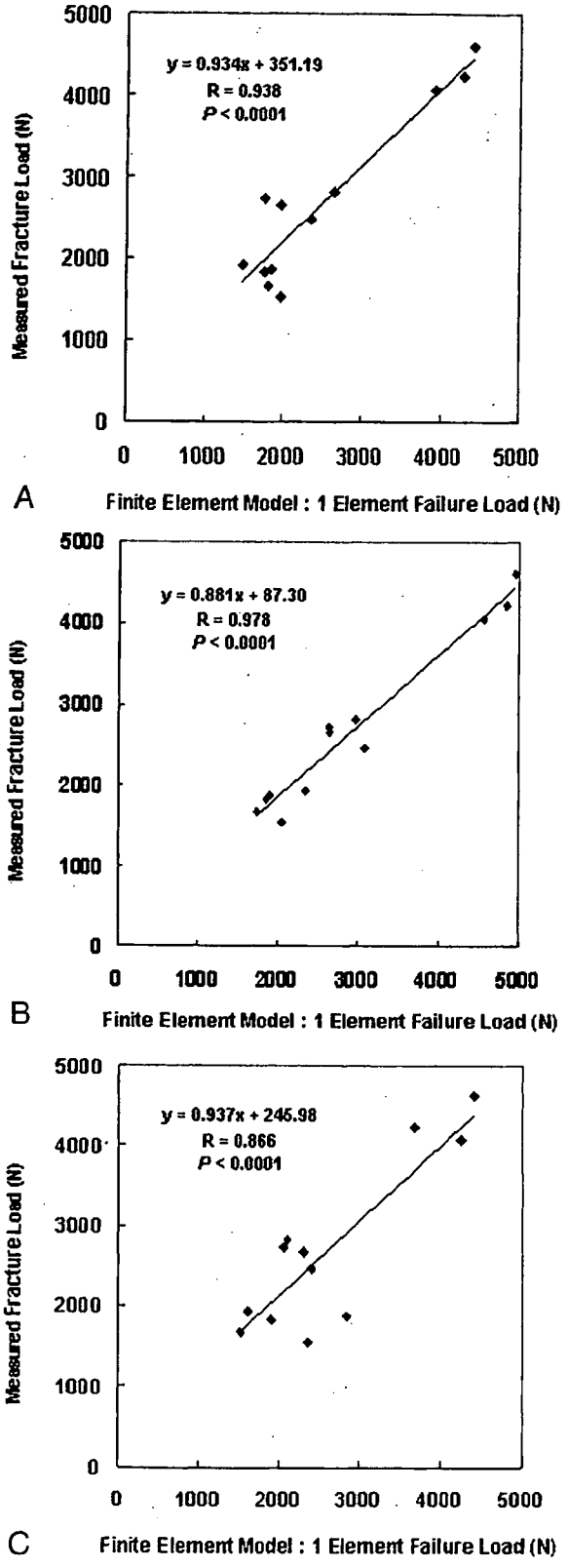

Figure 2. The measured fracture load *versus* the fracture load predicted by the finite element model (FEM). **A**, FEM with-1 mm tetrahedral elements. **B**, FEM with-2 mm tetrahedral elements. **C**, FEM with 3-mm tetrahedral elements. Strong correlations (r > 0.90) were obtained with elements of 1 mm and 2 mm in size, while a moderate correlation (r = 0.866) was obtained with 3-mm elements.

0.937 (Figure 2C). There was a strong linear correlation between the fracture load predicted by the 1 mm element model and that by the 2 mm (r = 0.959, $P < 0.0001$), and the slope of the regression line was 0.868. With the 1 mm and 3 mm models, the correlation was slightly weaker (r = 0.912, $P < 0.0001$), and the slope of the regression line was 0.839. With the 2 mm and 3 mm models, the correlation was much weaker (r = 0.878, $P < 0.0001$), and the slope of the regression line was 0.730.

In the convergence study, total strain energy decreased by 9.1% (4.0%–22.9%), with an increase of the element size from 1 mm to 1.4 mm. With an increase from 1.4 mm to 2 mm, it decreased by 10.0% (6.5%–17.3%), and decreased by 9.5% (2.9%–13.2%) from 2 mm to 3 mm. With an increase from 3 mm to 4.5 mm, total strain energy increased in some vertebrae although it decreased by an average of 38.6%.

In Vivo *Assessment of Lumbar Vertebral Strength*

The 78 women enrolled in the study had a mean age of 74.4 ± 5.6 years, a mean height of 148.4 ± 6.0 cm, and a mean weight of 50.3 ± 7.7 kg. The measured BMD of the lumbar spine was 0.808 ± 0.181 g/cm^2 and the strength of L2 predicted by the model was 2154 ± 685 N.

The subjects were classified into 5-year age groups, as summarized in Table 1. Height and vertebral strength showed a significant decrease in the older age groups, but weight and BMD did not change significantly (Kruskal-Wallis test, $P < 0.05$).

Next, the subjects were classified on the basis of prior vertebral fracture. Among the 78 women, 42 did not have any vertebral fractures (nonfracture group) and 36 subjects already had vertebral fractures (fracture group). Thus, vertebral fractures were present in 46.1% of the total study population. The characteristics of the 2 groups are summarized in Table 2. The nonfracture group was significantly younger than the fracture group (Mann-Whitney *U* test, $P < 0.001$). Height ($P < 0.05$) and weight ($P < 0.005$) were significantly greater in the nonfracture group than in the fracture group.

The average spinal BMD of the nonfracture group was 0.849 ± 0.146 g/cm^2, which was greater than that of the fracture group at 0.759 ± 0.207 g/cm^2 ($P < 0.05$) (Figure 3). The predicted vertebral strength of L2 was 2489 ± 580 N in the nonfracture group, which was greater than in the fracture group at 1764 ± 588 N ($P < 0.0001$) (Figure 3). The L2 strength to weight ratio was 4.80 ± 1.20 in the nonfracture group, and this was significantly greater than in the fracture group at 3.77 ± 1.36 ($P < 0.005$) (Figure 4).

■ Discussion

Assessing vertebral strength by using the FEM has been difficult because of the complex geometry, elastoplasticity, and thin cortical shell of the vertebra. The vertebrae have an elaborate architecture and geometry with curved surfaces, which cannot be modeled properly by using

Table 1. Summary of the Subjects' Height, Weight, BMD, and Analyzed Vertebral Strength (Mean ± SD)

Age (yr)	N	Height (cm)	Weight (kg)	BMD (g/cm^2)	Vertebral Strength (N)
60–64	6	153.5 ± 4.5	54.0 ± 6.1	0.850 ± 0.180	2592 ± 497
65–69	10	152.3 ± 7.8	50.9 ± 8.2	0.848 ± 0.112	2665 ± 528
70–74	21	148.1 ± 5.0	51.3 ± 7.4	0.744 ± 0.169	2050 ± 752
75–79	26	147.8 ± 6.2	48.5 ± 8.7	0.800 ± 0.200	2069 ± 706
80–85	15	145.1 ± 3.8	50.3 ± 6.3	0.867 ± 0.191	1933 ± 512

8-noded hexahedral elements. Previous mechanical tests have shown that there is a difference between the tensile and compressive strength of bone,[16–18] with compressive strength showing nonlinear behavior. Therefore, a nonlinear FEM should be used to predict the clinical fracture load. The cortical shell of each vertebra is estimated to have a thickness of approximately 0.4 mm.[12–14] In comparison, the resolution of clinically available CT scanners is fairly low, with a pixel spacing of larger than 0.25 mm. This means that the currently available CT data do not allow the thin cortical shell to be precisely modeled. The cortical thickness tends to be overestimated and its density is underestimated.[19,20] Therefore, it is necessary to construct a thinner model cortical shell from non-CT data. Shell elements of triangular plates with a uniform thickness of 0.4 mm were used to construct a cortical shell.

The characteristics of the present FEM in this study were as follows: adoption of the tetrahedral elements to model the surface curvature of the entire vertebra, utilization of nonlinear analysis to match the elastoplasticity of the vertebra during compression, and construction of a cortical shell as the surface of the model. It has been reported that the thin cortex of a vertebra contributes 12%–75% to its overall strength and the contribution of the cortex is estimated to be significantly larger in osteoporotic individuals.[21,22] Thus, the importance of the strength of the cortical shell should be taken into consideration when predicting the fracture load for osteoporosis patients.

The limitation of our model is that the cortical shell was treated as a homogenous material because the pixels of CT scans were too large to model the thin cortex. In addition, with the limited resolution of currently available CT scanners, the microarchitecture of the bone cannot be precisely assessed. Micro-CT and synchrotron micro-CT can visualize bone microstructure.[23] Therefore, an FEM based on micro-CT data may show more accurate simulation because it would be possible to model a cortical shell with heterogeneous properties and also to assess the microarchitecture. However, obtaining micro-CT scans of a whole vertebra *in vivo* would be impossible with the currently available scanners. Also, use of thinner CT slices to obtain images leads to more radiation exposure. To decrease radiation exposure for clinical use, somewhat thicker slices would be more appropriate.

Table 2. Background of the Subjects in No Fracture Group and Fracture Group

Group	N	Age (yr)	Height (cm)	Weight (kg)
No fracture group	42	72.3 ± 5.7	149.9 ± 5.7	52.6 ± 7.4
Fracture group	36	76.8 ± 4.6	146.6 ± 6.0	47.8 ± 7.3

We assessed 3 models each with a different element size of 1 mm, 2 mm, and 3 mm. With an element size of 1 mm and 2 mm, the correlation between the fracture load predicted by the FEM and that measured experimentally was very strong ($r > 0.90$). With an element size of 3 mm, the correlation was slightly weaker ($r < 0.90$). Although all of 3 FEM were generated using CT data obtained with a 1 mm slice thickness, these results suggested that the elements with a size of 1 mm or 2 mm could be used to accurately predict the fracture load. There was a stronger correlation ($r = 0.978$) with 2 mm tetrahedral elements than with either 1 mm or 3 mm elements. The correlation of the fracture load between the prediction and the experiment was better than that in the previous FEM studies ($r = 0.89–0.95$).[24–27] The slope of the regression line obtained with 2 mm tetrahedral elements was 0.881, which was also better than that in the previous FEM studies (0.569–0.86).[24–27] The previous FEM studies had failed to model the surface curvature of the vertebra, match the elastoplasticity of the vertebra, or model a cortical shell. These results indicated that our FEM predicted compressive vertebral strength more accurately.

The correlation between the fracture load with 1 mm and 2 mm elements ($r = 0.959$) was stronger than both of the correlations between 1 mm and 3 mm ($r = 0.912$), and between 2 mm and 3 mm ($r = 0.878$). The slope of the regression line relating 1 mm and 2 mm (0.868) was also better than that relating 1 mm and 3 mm (0.839), and that relating 2 mm and 3 mm (0.730). These results indicated that the prediction by the FEM with the 1 mm and 2 mm elements achieved more accurate result than the 3 mm elements.

The results obtained by the convergence study with the 1 mm, 1.4 mm, 2 mm, 3 mm, and 4.5 mm models suggested the model with 1 mm elements was the most accurate among the 5 models. However, the 2 mm model was thought to achieve sufficiently accurate prediction compared with the 1 mm model. In the previous FEM study using the models with 8-noded hexahedral elements, stiffness of the model with $3 \times 3 \times 3$ mm^3 elements was on average only 4% greater than that with

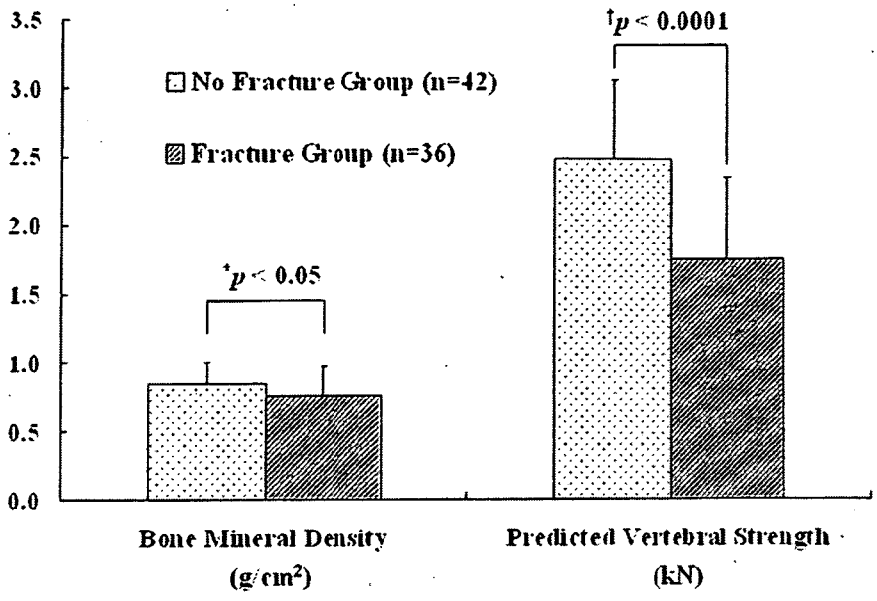

Figure 3. Bone mineral density of the lumbar spine (L2–L4) and predicted vertebral strength of the L2 vertebra in the nonfracture group (n = 42) and in the fracture group (n = 36). The error bars represent one standard deviation from the mean. Bone mineral density of the nonfracture group was greater than that of the fracture group. The difference was significant ($P < 0.05$). Predicted vertebral strength in the nonfracture group was also significantly ($P < 0.0001$) greater than that of the fracture group.

$1 \times 1 \times 1.5$ mm^3 elements, and there was a high correlation between the stiffness and the experimentally measured ultimate strength values in both $3 \times 3 \times 3$ mm^3 element model ($r^2 = 0.94$) and $1 \times 1 \times 1.5$ mm^3 element model ($r^2 = 0.92$).[28]

Based on these *in vitro* data, an *in vivo* study was performed using CT scans with a 2-mm slice thickness and a nonlinear FEM with an element size of 2 mm. There have been few reports about predicting vertebral strength *in vivo*, although some authors have assessed vertebral strength *in vitro* by mechanical testing. In the elderly, McBroom *et al* reported that among 10 specimens from subjects with an average age of 78 years, the average failure load for the L1 vertebral body was 3160 ± 424 N and it was 3385 ± 485 N for L3.[3] Eckstein *et al* reported that the average failure load for L3 was 3016 ± 149 N when they tested 102 specimens from the subjects with an average age of 80.6 years.[29] These 2 reports included both men and women. In the present study, however, all of the subjects were Japanese women. This might be one of the reasons why our predicted vertebral strength was smaller than that reported elsewhere.

The limitation in our study was that the prediction was made under a uniaxial compressive loading condition. In an *in vivo* situation, the loading and boundary conditions are completely different. However, one of the advantages of FEM simulation is that it allows us to set an arbitrary load magnitude or direction to simulate loading in various activities of daily living. If predicted strength by FEM was proved to be accurate in a uniaxial compressive loading condition, we could assume that we might be able to apply this method to predict accurately the strength under various other loading and boundary conditions. Nevertheless, the accuracy of our method in predicting strength under different loading and boundary conditions should be validated by conducting another mechanical testing and it would be one of our assignments in the future study.

In this study, the vertebral strength predicted by FEM could detect preexisting vertebral fractures better than

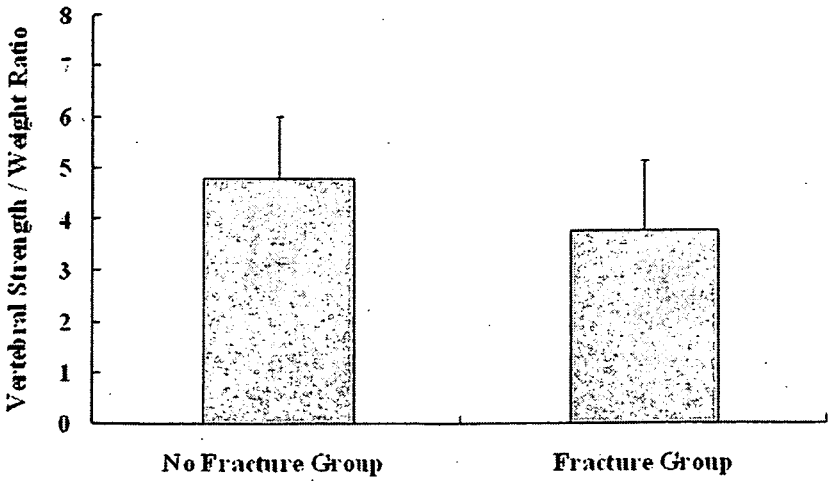

Figure 4. The ratio of L2 vertebral strength to weight in the nonfracture group (n = 42) and in the fracture group (n = 36). The difference was also significant ($P < 0.005$).

BMD. CT-based FEM assesses bone geometry and heterogeneous bone mass distribution as well as the BMD. It is hoped that CT-based FEM will become useful for estimating the risk of vertebral fracture in osteoporotic individuals.

■ Key Points

- *In vivo* assessment of lumbar vertebral strength in elderly Japanese women was performed using a CT-based nonlinear finite element model that was established and initially evaluated *in vitro*.
- The average L2 vertebral strength of the 78 subjects was 2154 ± 685 N according to this model.
- The present FEM could detect preexisting vertebral fracture more accurately than measurement of the bone mineral density.

References

1. Melton LJ. Epidemiology of spinal osteoporosis. *Spine* 1997;22(suppl):2–11.
2. Mosekilde L, Bentzen SM, Ortoft G, et al. The predictive value of quantitative computed tomography for vertebral body compressive strength and ash density. *Bone* 1989;10:465–70.
3. McBroom RJ, Hayes WC, Edwards WT, et al. Prediction of vertebral body compressive fracture using quantitative computed tomography. *J Bone Joint Surg Am* 1985;67:1206–14.
4. Brinckmann P, Biggemann M, Hilweg D, et al. Prediction of the compressive strength of human lumbar vertebrae. *Clin Biomech* 1989;4(suppl):1–27.
5. Edmondston SJ, Singer KP, Day RE, et al. In-vitro relationships between vertebral body density, size and compressive strength in the elderly thoracolumbar spine. *Clin Biomech* 1994;9:180–6.
6. Cheng XG, Nicholson PH, Boonen S, et al. Prediction of vertebral strength in vitro by spinal bone densitometry and calcaneal ultrasound. *J Bone Miner Res* 1997;12:721–8.
7. Eriksson SA, Isberg BO, Lindgren JU. Prediction of vertebral strength by dual photon absorptiometry and quantitative computed tomography. *Calcif Tissue Int* 1989;44:243–50.
8. Myers BS, Arbogast KB, Lobaugh B, et al. Improved assessment of lumbar vertebral body strength using supine lateral dual-energy x-ray absorptiometry. *J Bone Miner Res* 1994;9:687–93.
9. Bjarnason K, Hassager C, Svendsen OL, et al. Anteroposterior and lateral spinal DXA for the assessment of vertebral body strength: comparison with hip and forearm measurement. *Osteoporosis Int* 1996;6:37–42.
10. NIH Consensus Development Panel on Osteoporosis Prevention D, and Therapy. Osteoporosis prevention, diagnosis, and therapy. *JAMA* 2001;285:785–95.
11. Imai K, Ohnishi I, Bessho M, et al. Nonlinear finite element model predicts vertebral bone strength and fracture site. *Spine* 2006;31:1789–94.
12. Silva MJ, Wang C, Keaveny TM, et al. Direct and computed tomography thickness measurements of the human, lumbar vertebral shell and endplate. *Bone* 1994;15:409–14.
13. Vesterby A, Mosekilde L, Gundersen HJ, et al. Biologically meaningful determinants of the in vitro strength of lumbar vertebrae. *Bone* 1991;12:219–24.
14. Mosekilde L. Vertebral structure and strength in vivo and in vitro. *Calcif Tissue Int* 1993;53(suppl):121–6.
15. Keyak JH, Rossi SA, Jones KA, et al. Prediction of femoral fracture load using automated finite element modeling. *J Biomech* 1998;31:125–33.
16. Keaveny TM, Wachtel EF, Ford CM, et al. Differences between the tensile and compressive strengths of bovine tibial trabecular bone depend on modulus. *J Biomech* 1994;27:1137–46.
17. Kopperdahl DL, Keaveny TM. Yield strain behavior of trabecular bone. *J Biomech* 1998;31:601–8.
18. Morgan EF, Keaveny TM. Dependence of yield strain of human trabecular bone on anatomic site. *J Biomech* 2001;34:569–77.
19. Dougherty G, Newman D. Measurement of thickness and density of thin structures by computed tomography: a simulation study. *Med Phys* 1999;26:1341–8.
20. Prevrhal S, Engelke K, Kalender WA. Accuracy limits for the determination of cortical width and density: the influence of object size and CT imaging parameters. *Phys Med Biol* 1999;44:751–64.
21. Faulkner KG, Cann CE, Hasegawa BH. Effect of bone distribution on vertebral strength: assessment with patient-specific nonlinear finite element analysis. *Radiology* 1991;179:669–74.
22. Rockoff SD, Sweet E, Bleustein J. The relative contribution of trabecular and cortical bone to the strength of human lumbar vertebrae. *Calcif Tissue Res* 1969;3:163–75.
23. Ito M. Assessment of bone quality using micro-computed tomography (micro-CT) and synchrotron micro-CT. *J Bone Miner Metab* 2005;23(suppl):115–21.
24. Silva MJ, Keaveny TM, Hayes WC. Computed tomography-based finite element analysis predicts failure loads and fracture patterns for vertebral sections. *J Orthop Res* 1998;16:300–8.
25. Martin H, Werner J, Andresen R, et al. Noninvasive assessment of stiffness and failure load of human vertebrae from CT-data. *Biomed Tech* 1998;43:82–8.
26. Liebschner MA, Kopperdahl DL, Rosenberg WS, et al. Finite element modeling of the human thoracolumbar spine. *Spine* 2003;28:559–65.
27. Crawford RP, Cann CE, Keaveny TM. Finite element models predict in vitro vertebral body compressive strength better than quantitative computed tomography. *Bone* 2003;33:744–50.
28. Crawford RP, Rosenberg WS, Keaveny TM. Quantitative computed tomography-based finite element models of the human lumbar vertebral body: effect of element size on stiffness, damage, and fracture strength predictions. *J Biomech Eng* 2003;125:434–8.
29. Eckstein F, Lochmüller EM, Lill CA, et al. Bone strength at clinically relevant sites displays substantial heterogeneity and is best predicted from site-specific bone densitometry. *J Bone Miner Res* 2002;17:162–71.

Prediction of strength and fracture location of the proximal femur by a CT-based nonlinear finite element method - Effect of load direction on hip fracture load and fracture site -

Masahiko Bessho, Isao Ohnishi, Takuya Matsumoto, Satoru Ohashi, Kenji Tobita, Juntaro Matsuyama, Kozo Nakamura
Orthopaedic Surgery, University of Tokyo, Tokyo, Japan
ohnishii-dis@h.u-tokyo.ac.jp

Introduction: The occurrence rate of hip fractures due to osteoporosis is rapidly increasing, representing one of the most serious and urgent social problems. We focused on a computed tomography-based finite element method (CT/FEM) to quantify structural strength, thereby developing a nonlinear CT/FEM to achieve accurate assessment of strength of the proximal femur [1]. The aim of this study was to investigate the effect of load direction on fracture risk of the proximal femur. For this purpose, we evaluated changes in magnitude of strength for the proximal femur with changes in load direction by analyzing the contralateral femur in patients with hip fracture using the nonlinear CT/FEM. We also verified changes in fracture risk by site. From these analyses, we identified load and boundary conditions that could increase risk of hip fracture and clarified that this could possibly cause the fracture types commonly seen in clinical situations.

Materials and Methods: Twenty eight femora in female patients with contralateral hip fracture (age: 80 - 91, average: 85.2)(femoral neck fracture: 13 patients, trochanteric fracture: 15 patients). The study protocol was approved by our ethics committee and the patients were enrolled after informed consent was given. Within 7 days after admission, axial CT images of the proximal femur were obtained (slice thickness: 3 mm, Aquilion Super 4, Toshiba Medical Systems Co., Tokyo, Japan) as well as scans of a calibration phantom. The CT data were transferred to a workstation and 3D finite element models were constructed from the CT data using Mechanical Finder (Research Center of Computational Mechanics Inc., Tokyo, Japan). Trabecular bone and the inner portion of cortical bone were modeled using 3 mm linear tetrahedral elements, while the outer cortex was modeled using 3 mm triangular plates (0.4 mm thick)[1]. On average, there were 75,212 tetrahedral elements and 4,103 triangular plates.

Force was applied to the femoral head at an angle γ to the shaft in the frontal plane and at an angle δ to the neck axis in the transverse plane (Fig. 1). For stance configuration (SC), γ and δ were set at 160° and 0°. For fall configuration (FC), γ and δ were set at 120° and 0° (FC1), 60° and 0° (FC2), 60° and 15° (FC3) or 60° and 45° (FC4), respectively [4, 5].

Materially nonlinear finite element analysis was performed by the Newton-Raphson method. Fracture was defined as occurring when at least one shell element failed. Fracture loads were predicted and sites at fracture risk were identified [1].

Correlations between predicted fracture load and load direction were investigated. Predicted fracture type was compared with contralateral actual fracture type.

Pearson's correlation analysis, Friedman test, Scheffe's post hoc test and Fisher's exact test were used for statistical analyses and the results were considered significant when p values were less than 0.05.

Results: The average predicted fracture loads for SC was 3080 N (standard deviation (SD): 551 N), 2210 N (SD: 606 N) for FC1, 1047 N (SD: 236 N) for FC2, 970 N (SD: 199 N) for FC3 and 700 N (SD: 167 N) for FC4, respectively.

The predicted fracture loads for SC were significantly higher than those for all fall configurations except for FC1 ($p < 0.001$).

In comparisons of predicted fracture loads for all fall configurations, loads were significantly higher for FC1 than for FC2, FC3 or FC4 ($p=0.02$, $p<0.001$, $p<0.001$, respectively).

The predicted fracture loads for FC2 were significantly higher than those for FC4 ($p < 0.001$). The predicted fracture loads for FC3 were significantly higher than those for FC4 ($p < 0.01$).The correlations of the predicted fracture loads for all configurations were shown on Table 1.

The predicted fracture sites located at sub-capital region in all patients for SC. The predicted sites located at trochanteric region in all patients for all fall loading configurations except for FC1. For FC1, the predicted sites located at sub-capital region in13 patients, but in 15 patients, they located at trochanteric region. For 20 patients, contralateral actual fracture type corresponded to predicted fracture type. Predicted fracture type corresponded significantly to contralateral actual fracture type ($p<0.01$).

Discussion: As δ increases, the fall tends to be directed more posteriorly. Falls in a posterolateral direction were thus indicated to increase fracture risk more than falls to the side. Each of the predicted fracture loads from various loading conditions displayed poor correlation with each other, even though most correlations were significant. Strength of the proximal femur should thus be evaluated under multiple loading conditions. Intertrochanteric fractures were predicted to occur under all fall loading conditions except FC1. Hirsch et al. reported that compressive force along the long axis of the femoral neck is necessary for femoral neck fractures to occur [6]. Mean neck-shaft angle of the femur is known to be 120°-130°, so FC1 was considered as the condition that could cause neck fractures. If we assume that no morphological differences exist between right and left femora in each patient [7], in all fall loading conditions except FC1, the loading condition would possibly be the only decisive factor for fracture type, irrespective of the morphological characteristics of each patient. Conversely, in FC1, fracture type might differ depending on morphological characteristics of each patient. Keyak et al. reported relationships between loading direction and magnitude of predicted fracture load [4]. However, they reported results from only 4 patients and statistical analyses were not conducted. In addition, they lacked information on predicted fracture sites. The present study could contribute to providing us with useful information for the establishment of effective measures to prevent hip fractures.

References: [1] Bessho et al. J Biomech 40: 1745-53, 2007 [2] Keyak et al., J Biomed Mater Res 28: 1329-36, 1994 [3] Keller et al., J Biomech 27: 1159-68, 1994 [4] Keyak et al., J Orthop Res 19: 539-44, 2001 [5] Fujii et al., Nippon Seikeigeka Gakkai Zasshi 61: 531-41, 1987 [6] Hirsch et al., J Bone Joint Surg Br 42: 633-40, 1960 [7] Boston et al., Injury 14: 207-10, 1982

Table 1. Correlations (r) of the predicted fracture loads for each loading configurations.

	SC	FC1	FC2	FC3	FC4
SC	-	n.s.	0.52	0.55	0.67
FC1	n.s.	-	0.55	0.55	0.49
FC2	0.52	0.55	-	0.88	0.67
FC3	0.55	0.55	0.88	-	0.81
FC4	0.67	0.49	0.67	0.81	-

n.s.: not significant

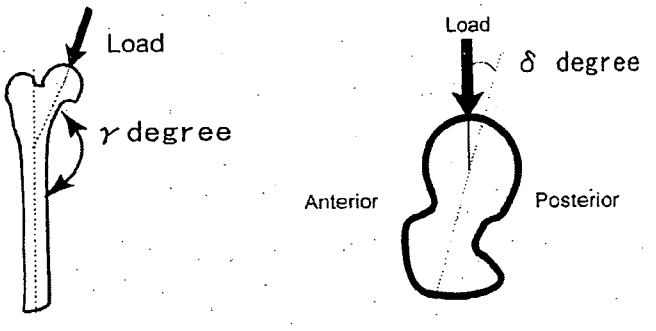

Fig. 1. Force direction

Prediction of strength and fracture location of the proximal femur by a CT-based nonlinear finite element method - Effect of load direction on hip fracture load and fracture site -

Masahiko Bessho, Isao Ohnishi, Takuya Matsumoto, Satoru Ohashi, Kenji Tobita, Juntaro Matsuyama, Kozo Nakamura
Orthopaedic Surgery, University of Tokyo, Tokyo, Japan
ohnishii-dis@h.u-tokyo.ac.jp

Introduction: The occurrence rate of hip fractures due to osteoporosis is rapidly increasing, representing one of the most serious and urgent social problems. We focused on a computed tomography-based finite element method (CT/FEM) to quantify structural strength, thereby developing a nonlinear CT/FEM to achieve accurate assessment of strength of the proximal femur [1]. The aim of this study was to investigate the effect of load direction on fracture risk of the proximal femur. For this purpose, we evaluated changes in magnitude of strength for the proximal femur with changes in load direction by analyzing the contralateral femur in patients with hip fracture using the nonlinear CT/FEM. We also verified changes in fracture risk by site. From these analyses, we identified load and boundary conditions that could increase risk of hip fracture and clarified that this could possibly cause the fracture types commonly seen in clinical situations.

Materials and Methods: Twenty eight femora in female patients with contralateral hip fracture (age: 80 - 91, average: 85.2)(femoral neck fracture: 13 patients, trochanteric fracture: 15 patients). The study protocol was approved by our ethics committee and the patients were enrolled after informed consent was given. Within 7 days after admission, axial CT images of the proximal femur were obtained (slice thickness: 3 mm, Aquilion Super 4, Toshiba Medical Systems Co., Tokyo, Japan) as well as scans of a calibration phantom. The CT data were transferred to a workstation and 3D finite element models were constructed from the CT data using Mechanical Finder (Research Center of Computational Mechanics Inc., Tokyo, Japan). Trabecular bone and the inner portion of cortical bone were modeled using 3 mm linear tetrahedral elements, while the outer cortex was modeled using 3 mm triangular plates (0.4 mm thick)[1]. On average, there were 75,212 tetrahedral elements and 4,103 triangular plates.

Force was applied to the femoral head at an angle γ to the shaft in the frontal plane and at an angle δ to the neck axis in the transverse plane (Fig. 1). For stance configuration (SC), γ and δ were set at 160° and 0°. For fall configuration (FC), γ and δ were set at 120° and 0° (FC1), 60° and 0° (FC2), 60° and 15° (FC3) or 60° and 45° (FC4), respectively [4, 5].

Materially nonlinear finite element analysis was performed by the Newton-Raphson method. Fracture was defined as occurring when at least one shell element failed. Fracture loads were predicted and sites at fracture risk were identified [1].

Correlations between predicted fracture load and load direction were investigated. Predicted fracture type was compared with contralateral actual fracture type.

Pearson's correlation analysis, Friedman test, Scheffe's post hoc test and Fisher's exact test were used for statistical analyses and the results were considered significant when p values were less than 0.05.

Results: The average predicted fracture loads for SC was 3080 N (standard deviation (SD): 551 N), 2210 N (SD: 606 N) for FC1, 1047 N (SD: 236 N) for FC2, 970 N (SD: 199 N) for FC3 and 700 N (SD: 167 N) for FC4, respectively.

The predicted fracture loads for SC were significantly higher than those for all fall configurations except for FC1 ($p < 0.001$).

In comparisons of predicted fracture loads for all fall configurations, loads were significantly higher for FC1 than for FC2, FC3 or FC4 ($p=0.02$, $p<0.001$, $p<0.001$, respectively).

The predicted fracture loads for FC2 were significantly higher than those for FC4 ($p < 0.001$). The predicted fracture loads for FC3 were significantly higher than those for FC4 ($p < 0.01$).The correlations of the predicted fracture loads for all configurations were shown on Table 1.

The predicted fracture sites located at sub-capital region in all patients for SC. The predicted sites located at trochanteric region in all patients for all fall loading configurations except for FC1. For FC1, the predicted sites located at sub-capital region in13 patients, but in 15 patients, they located at trochanteric region. For 20 patients, contralateral actual fracture type corresponded to predicted fracture type. Predicted fracture type corresponded significantly to contralateral actual fracture type ($p<0.01$).

Discussion: As δ increases, the fall tends to be directed more posteriorly. Falls in a posterolateral direction were thus indicated to increase fracture risk more than falls to the side. Each of the predicted fracture loads from various loading conditions displayed poor correlation with each other, even though most correlations were significant. Strength of the proximal femur should thus be evaluated under multiple loading conditions. Intertrochanteric fractures were predicted to occur under all fall loading conditions except FC1. Hirsch et al. reported that compressive force along the long axis of the femoral neck is necessary for femoral neck fractures to occur [6]. Mean neck-shaft angle of the femur is known to be 120°-130°, so FC1 was considered as the condition that could cause neck fractures. If we assume that no morphological differences exist between right and left femora in each patient [7], in all fall loading conditions except FC1, the loading condition would possibly be the only decisive factor for fracture type, irrespective of the morphological characteristics of each patient. Conversely, in FC1, fracture type might differ depending on morphological characteristics of each patient. Keyak et al. reported relationships between loading direction and magnitude of predicted fracture load [4]. However, they reported results from only 4 patients and statistical analyses were not conducted. In addition, they lacked information on predicted fracture sites. The present study could contribute to providing us with useful information for the establishment of effective measures to prevent hip fractures.

References: [1] Bessho et al. J Biomech 40: 1745-53, 2007 [2] Keyak et al., J Biomed Mater Res 28: 1329-36, 1994 [3] Keller et al., J Biomech 27: 1159-68, 1994 [4] Keyak et al., J Orthop Res 19: 539-44, 2001 [5] Fujii et al., Nippon Seikeigeka Gakkai Zasshi 61: 531-41, 1987 [6] Hirsch et al., J Bone Joint Surg Br 42: 633-40, 1960 [7] Boston et al., Injury 14: 207-10, 1982

Table 1. Correlations (r) of the predicted fracture loads for each loading configurations.

	SC	FC1	FC2	FC3	FC4
SC	-	n.s.	0.52	0.55	0.67
FC1	n.s.	-	0.55	0.55	0.49
FC2	0.52	0.55	-	0.88	0.67
FC3	0.55	0.55	0.88	-	0.81
FC4	0.67	0.49	0.67	0.81	-

n.s.: not significant

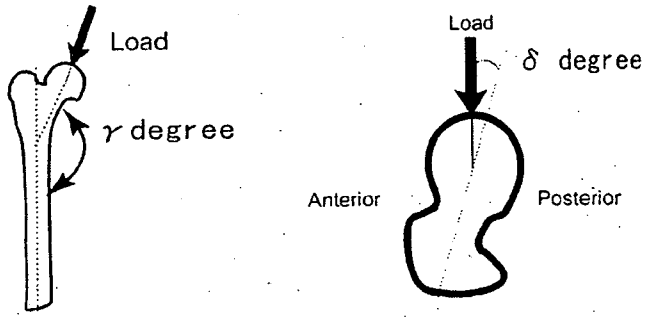

Fig. 1. Force direction

AN ASYMMETRICAL THREAD PROFILE EXTERNAL FIXATION PIN HAS HIGHER PULLOUT STRENGTH THAN A SYMMETRICAL THREAD PIN

Satoru Ohashi, Isao Ohnishi, Juntaro Matsuyama, Masahiko Bessho, Takuya Matsumoto, Kozo Nakamura
Department of Orthopaedic Surgery, Faculty of Medicine, University of Tokyo, Tokyo, Japan
soohashi-tky@umin.ac.jp

Introduction: One of the common complications in external fixation is pin loosening, which is suggested to be caused by stress concentration at the pin-bone interface [1, 4]. It could be minimized by utilizing improved thread profile design of the pins [4]. There have been several studies investigating the relationship between pin thread profile and pin pullout strength or pin-bone interface stress by conducting mechanical testing [2, 5] or by finite element (FE) method [3]. The thread configurations, however, in those studies were all symmetrical and no study has investigated mechanics of asymmetrical thread pins. We hypothesized mechanical performance of asymmetrical thread profile pins could be different from that of symmetrical pins. The purpose of this study was to investigate the mechanical performance of the asymmetrical pins by conducting pullout testing. Concurrently, three-dimensional FE models for the simulation of the pullout testing were created, thereby investigating the energy and stress distributions at the pin-bone interface using FE analysis.

Materials and Methods: Based on ISO 9268: 1988, we manufactured three different thread profile screw pins with an outer diameter of 6mm, an inner diameter of 4.8mm and a pitch of 1.8mm made of 6 Aluminum 4 Vanadium Titanium alloy. One had symmetrical thread and the other two were asymmetrically threaded. For the mechanical testing, 6mm thick epoxy-sheets (E-glass-filled Epoxy Sheet, 3001-04, Sawbones®, Pacific Research Laboratories, Inc., Vashon, WA) were used as cortical bone models. Pre-drilling the model using a 4.5 mm diameter drill bit was preceded before the pins were inserted with self-tapping technique. 6 pins were tested for each thread type. Pullout testing was conducted using a metal stopper with a 14 mm diameter round hole to restrain upward displacement of the bone model. Pins were pulled up with a mechanical testing machine (Servopulser EHF-LB5KN-10L, Shimazu, Kyoto, Japan) at a cross head speed of 0.03 mm/sec, based on the ASTM, F543-02 guidelines. The load was measured by a load cell (SCL-5KN, Shimazu, Kyoto, Japan) with a range of 7.5 kN. The pullout strength was defined as the ultimate strength achieved and described as a mean and a standard deviation (SD). The results of the mechanical tests were statistically analyzed by the analysis of variance. The differences were considered significant when p-values were less than 0.05.

Pullout testing simulation was performed using a FE method for the asymmetrical thread pins under a condition identical to the mechanical testing. Three-dimensional surface data in a computer assisted designing format for the screw pins and the cortical bone model were put into the mesh generation software (ANSYS ICEM CFD 5.1, Ansys Inc. Canonsburg, PA). FE mesh models of the pins and the bone model were created using tetrahedral elements with a variable side length of 0.5 to 1.0 mm by the oct-tree algorithm method. The average numbers of nodes and elements were 23,000 and 120,000, respectively. These meshes were imported into a finite element analysis software (Mechanical Finder software, RCCM, Tokyo, Japan). Young's moduli of the screws and the bone model were assumed to be isotropic, and assigned as that of 6 Aluminum 4 Vanadium Titanium (109.4 GPa) for the pins and that of the epoxy-sheet (12.4 GPa) used in the mechanical testing. Poisson's ratio was set as 0.28 for the pins and 0.4 for the bone model. A simulated uniaxial pullout load was applied at the end of the pin along its long axis. In order to simulate the contact interfacial characteristics between the screw pin and the bone model, node-on-node gap elements were created on the interface nodes. Virtual length of the gap elements was set as 0.1mm. Young's modulus of the gap element was set as the mean modulus of the pin and that of the bone model. The friction coefficient was set as 0.3. Linear analysis was performed with a pullout load of 4000 N. The average computing time was about 10 h. In post processing analysis, the pin–bone interface strain energy and stress concentration were assessed by analyzing the maximum strain energy density and the maximum equivalent stress (von Mises stress). The maximum strain energy density and the maximum equivalent stress were defined as the maximum values of the strain energy density and the equivalent stress of all bone elements.

Results: The measured pullout strength for the type A pin was significantly higher than that for the symmetrical thread pin and the type B pin ($p < 0.0001$). The maximum strain energy density and the maximum equivalent stress obtained from FE analysis for each pin were listed on Table 2. The maximum strain energy density and the maximum equivalent stress for the type A pin was the smallest of all pins. Each bone element with the maximum strain energy density or the maximum equivalent stress located at the pin-bone interface of each pin-bone complex model.

Discussion: From the results of the FE analysis, it was assumed the lower energy or stress concentration at the pin-bone interface of type A pin contributed to its significantly higher pullout strength in the mechanical testing. By adopting the asymmetrical thread pins, we may be able to enhance fixation by external fixators, thereby lowering the risk of pin loosening.

References: 1. Aro HT et al, J Trauma, 35, 1993; 2. Halsey D et al, Clin Orthop Relat Res, 278, 1992; 3. Hansson S et al, J Biomech, 36, 2003; 4. Huiskes R et al, J Orthop Res, 3, 1985; 5. Liu J et al, Clin Orthop Relat Res, 310, 1995

Acknowledgements: This work was funded by the grant in aid of the 15th Medical Frontier Project of Pharmaceuticals and Medical Devices Agency (PMDA) of Japan.

	Type A pin	Symmetrical pin	Type B pin
Pullout strength (N)	4698.3 ± 44.6	4333.3 ± 46.0	4281.3 ± 95.0
Maximum strain energy density (MJ/m3)	2.28	4.12	3.83
Maximum equivalent stress (MPa)	179.69	402.13	379.84

Values are described as the mean ± standard deviation.

The total angle of the thread tip was 45 degrees for all pins. The angle β and γ are defined as shown on the scheme and set as 22.5° and 22.5° for the symmetrical thread pin, 40.0° and 5.0° for type A pin, and 5.0° and 40.0° for type B pin, respectively.

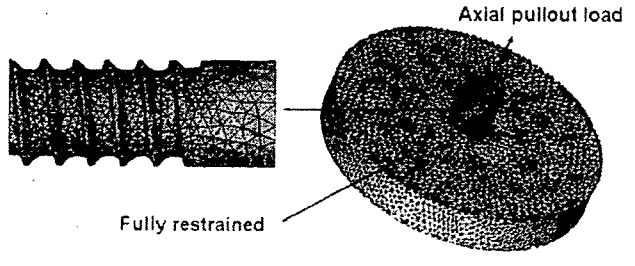

Each of the screw models was inserted in the center of a circular disk with a thickness of 6 mm and a diameter of 40mm, which simulated the cortical bone model.

75

3次元CT画像とCADデータを用いた手術シミュレーションの試み

Preoperative simulation using 3 dimensional CT and CAD datum

○松本 卓也、大西五三男、飛田 健治、大橋　暁、別所 雅彦、中村 耕三

東京大学医学部整形外科

長管骨変形治癒合に対して種々の創外固定器による変形矯正が幅広く行われている。矯正の為に創外固定器上にヒンジを設置、もしくはバーチャルヒンジを設定してレントゲンを基にした正面・側面の2次元変形角度の矯正を行う回旋変形の評価はCT画像を必要とする。2006年第19回本学会において大西らにより発表されたユニバーサル・バー・リンク機構を有する片側式創外固定器(UBL)を用いた変形矯正術前計画に際し、CTデータより3次元構築した患者固有の3次元骨モデルを用いた3次元変形矯正術前計画/手術シミュレーションを試みた。撮影したCT dicomデータを使用し、レキシー(株)のZed Viewを用い骨領域を抽出、患者固有の骨STLモデルを作成。同社との産学協同で開発したソフトを用い、作成した3Dモデルから設定したCORAを参照し、骨切面を設定。UBLのCADデータを用いて、手術手技どおりに近位部にピンを設置、UBLの各ヒンジの角度設定を行い遠位ピン刺入部の最適な設置部位を決定し、設置。設定完了することにより手術シミュレーションが完了する。骨切により分離した骨片は各ヒンジの角度を変化させることによりCORAを中心に動き、術前計画どおりに健側同様のベクトル角度をとるように移動する。STLモデルはコンピュータ画面上で自由に動かせるため多方面から変形を評価する事ができるため2Dのレントゲン写真だけでは評価が難しい回旋変形も容易に評価できる。本ソフトを臨床応用し、より高精度に変形矯正を行いたい。

3次元CT画像を基にした管骨変形評価法

Deformity Evaluation of the Tubular Bone Using 3D CT Image

東京大学医学部整形外科 ○飛田健治、大西五三男、別所雅彦、松本卓也
大橋暁、中村耕三

背景：長管骨の変形手術の術前計画は精確性を要する。Paleyら(1992)による術前計画法は正面･側面の単純レントゲン写真から変形量、変形中心(CORA)を求める方法を確立したが、レントゲンのみでは精確な術前計画は難しく、再現性を欠く。村瀬ら(2006, 2007)は3次元ＣＴの健側から患側の鏡像イメージを作成しこれを重ね合わせることで変形量を計測し術前計画を行った。しかし、両側の長管骨に変形を伴う場合はこの方法は行えない。

目的：ＣＴを用いた3次元的アライメント定量評価法を開発する。

方法：撮影したＣＴ dicomデータより骨領域を抽出し、3次元ＳＴＬモデルを作成。開発した専用ソフトウェアを用い、プログラムの中の特徴点を算出する機能を作り、画面上にてクリックする。①骨頭中心②大転子③小転子④内顆⑤外顆の５点を候補特徴点とし、これらを結ぶ線分の成す角で最小のものを３次元角度とした。また、特徴点の算出、角度計測にはＭＰＲ機能を搭載し決定した。先ずは大

腿骨上で3次元のLateral proximal femoral angle(以下PFA)、Lateral distal femoral angle （以下DFA)と回旋角を算出した。回旋角はレントゲンでの評価は困難であるが、3次元CT上では容易である。

症例:31歳男性。右大腿骨骨折後変形治癒にて当院紹介受診。3次元的変形量はPFA、DFA、回旋角の健側角/患側角はそれぞれ102.30°/78.88°，83.40°/90.50°，16.16°/51.06° であった。

今後: 今後症例を増やし有用性をさらに検討する。

31

Universal-Bar-Link 創外固定器を用いた変形矯正における固定器設置位置・角度の誤差許容範囲の検討

Evaluation of mounting error tolerance for spatial position and posture in the deformity correction using the Universal-Bar-Link external fixator

○大橋 暁[1]、大西五三男[1]、池澤 賢治[2]、佐久間一郎[2]、松本 卓也[1]、中村 耕三[1]

[1] 東京大学整形外科、[2] 東京大学工学部新領域創成科学研究科

【背景】我々は、骨延長・変形矯正のための新規の片持ち式創外固定器であるUniversal-Bar-Link創外固定器(以下UBL)を開発し、本学会にて報告した。この創外固定器は、リンク機構結合部の回転軸を調節することで骨が仮想球中心を中心とした球運動を行うことで角度矯正を、また、カーボンシャフトに沿って移動することで骨延長を実現するものである。そのため、変形骨の変形中心と仮想球中心位置が一致すること(以下Position)、Mechanical Axisに対してカーボンシャフトを平行に配置すること(以下Posture)、以上の2点についてUBL創外固定器を設置する際に正確に行うことが重要である。本研究ではUBL創外固定器のPositionとPostureの許容される設置誤差を本創外固定器専用に開発したナビゲーションソフトにてシミュレーションし検討した。【方法】正常骨モデルおよび大腿骨重度変形モデルをモデル骨にて作製し、CT画像を基にそれぞれの表面形状モデルを作成した。変形骨モデルに対してCORAを算出し、理想的にUBL創外固定器を取付けた状態で正常骨を参照しながら整復シミュレーションを行い(以下NL)、整復後のmechanical lateral distal femoral angle(以下mLDFA)、lateral proximal femoral angle(以下LPFA)を測定した。また、UBL設置のPositionを三次元空間上6方向にそれぞれ5mmずつ偏位させた整復シミュレーション(以下Position)、UBL設置のPostureを正面像・側面像において5°傾けた整復シミュレーション(以下Posture)をNLと同様に行い、mLDFA、LPFAを測定しNLの測定値との差をそれぞれ算出した。【結果】PositionとNLの差の絶対値(平均±標準偏差)は、mLDFA：0.18±0.12°(最小0.05°、最大0.35°)、LPFA：0.18±0.13°(最小0.06°、最大0.36°)であった。また、PostureとNLの差の絶対値は、mLDFA：1.46±0.67°(最小0.69°、最大1.93°)、LPFA：0.51±0.08°(最小0.46°、最大0.60°)であった。【考察】Paleyらの報告ではmLDFA、LPFAは正常値が共に85°～90°であり、±約2°の残存角度は許容されると考えられる。今回の結果から、UBLの目標からの設置位置・角度誤差はそれぞれ5mm・5°以内であれば臨床的に許容範囲内であると考えられた。この許容範囲は手術において比較的容易に達成できるものであり、UBL創外固定器は臨床的に十分有用であると考えられる。